Catalysis Letters (2020) 150:881–887
https://doi.org/10.1007/s10562-019-02944-y

Selective Liquid Phase Hydrogenation of Benzaldehyde to Benzyl Alcohol Over Alumina Supported Gold

Yufen Hao[1] · Chiara Pischetola[1] · Fernando Cárdenas-Lizana[1] · Mark A. Keane[1]

Received: 11 May 2019 / Accepted: 9 August 2019 / Published online: 30 September 2019

Abstract

We report for the first time 100% benzyl alcohol yield from the liquid phase ($T = 353$ K, $P = 9$ bar) hydrogenation of benzaldehyde over Au/Al_2O_3. Under the same reaction conditions, a benchmark Pt/Al_2O_3 catalyst promoted the formation of toluene and benzene as hydrogenolysis by-products. Reaction kinetics was subjected to a Hammett treatment and the reaction constant ($\rho = 0.9$) was found to be consistent with a nucleophilic mechanism. A solvent (alcohol, water and alcohol + water) effect is demonstrated and ascribed to competitive adsorption where solvation by polar (water) facilitates benzaldehyde activation.

Graphic Abstract

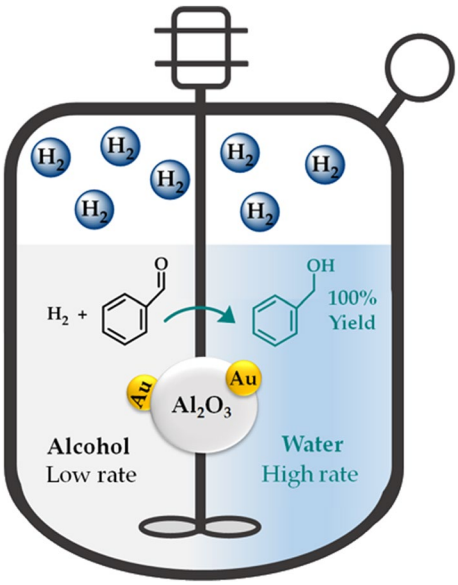

Keywords Selective hydrogenation · Benzaldehyde · Benzyl alcohol · Water as solvent · Au/Al_2O_3 · Pt/Al_2O_3

1 Introduction

The production of benzyl alcohol by the selective reduction of benzaldehyde is an important commercial process with multiple applications as solvent for inks, paints and lacquers [1]. Oxide supported Ru [2], Pd [3, 4], Ni [5, 6] Cu [7] and Pt [8, 9] catalysts have been employed, typically in batch liquid phase at high pressure (20–40 bar) [1, 2, 5, 8, 10,

✉ Fernando Cárdenas-Lizana
F.CardenasLizana@hw.ac.uk

[1] Chemical Engineering School of Engineering and Physical Sciences, Heriot-Watt University, Edinburgh EH14 4AS, Scotland, UK

11]. The target of 100% benzyl alcohol yield (Scheme 1, path I) remains a challenge as undesired hydrogenolysis (to toluene and/or benzene, paths II–V [12]) is difficult to circumvent with reported alcohol yields in the 40–75% range [2–6, 9, 13]. Application of Au in hydrogenation, though less developed than use in oxidation, has been the focus of recent research [14–19]. In their review, Hari and Yaakob [20] established the potential of Au for selective liquid phase hydrogenation with enhanced alcohol selectivity in the conversion of aldehydes such as crotonaldehyde [21] and citral [22]. We provide here the first reported application of (Al_2O_3) supported Au in the liquid phase hydrogenation of benzaldehyde.

Gold delivers lower activity when compared with conventional transition metal catalysts due to a less effective activation/dissociation of H_2 [23, 24]. Hydrogenation activity in liquid phase operation can be influenced by the solvent [25]. This has been related to differences in dielectric constant (ε) [26–28], bonding capacity (α) [28, 29] and H_2 solubility [26]. Aramendía et al. [30] and Bertero et al. [27] found that the rate of acetophenone hydrogenation decreased with increasing ε of C_1–C_3 alcohols, which they ascribed to solvation effects that influenced reactant adsorption. On the other hand, Wan et al. [28] observed an increased hydrogenation rate with increasing α, linked to interaction between

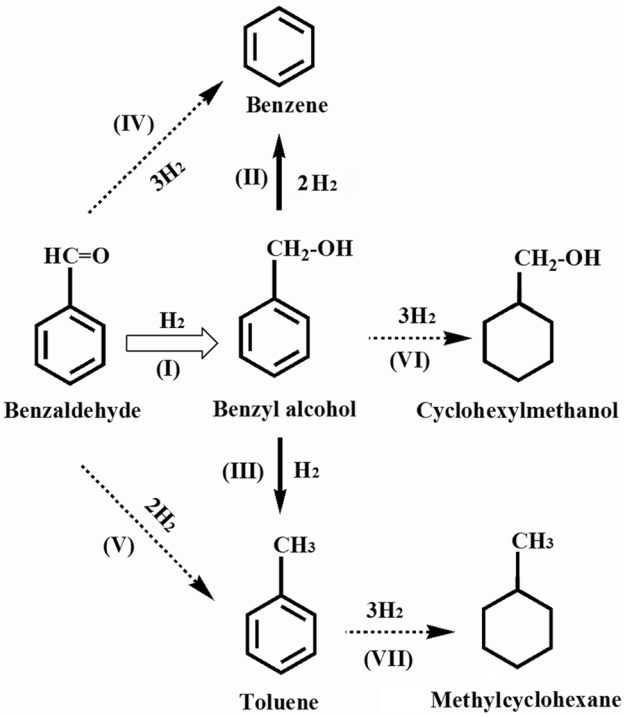

Scheme 1 Reaction pathway associated with benzaldehyde hydrogenation; pathway to the target alcohol (open arrow), by-products detected in this work (solid arrows) and reported in the literature [12] (dashed arrows)

protic solvents and 2-butanone by hydrogen bonding that lowered the activation energy barrier. Drelinkiewicza et al. [26] concluded that acetophenone hydrogenation was more influenced by solvent polarity than H_2 solubility. Organic solvents such as ethanol [3, 4, 9, 10, 13], dioxane [5] and alkanes (*n*-octane [3] and dodecane [31]) have been used in the liquid phase hydrogenation of benzaldehyde. Water as a benign green reaction medium has not been considered to any great extent. It is nonetheless worth flagging the work of Wang and co-workers [32] who demonstrated higher activity in the chemoselective hydrogenation of α, β-unsaturated carbonyl compounds over Au/CeO_2 in water relative to organic solvents (ethanol, isopropanol, dioxane and cyclohexane).

In this work, we examine the role of solvent (*n*-pentanol, *n*-butanol, ethanol, H_2O and ethanol + H_2O mixtures) in determining benzaldehyde hydrogenation over Au/Al_2O_3. We have targeted 100% benzyl alcohol yield as an objective. The effect of *para*-positioned substituents (–OCH_3, –CH_3, –CH_2CN and –CN) on rate has also been considered. Given the established application of supported Pt in benzaldehyde hydrogenation [8, 10, 11], we employed a commercial Pt/Al_2O_3 as a suitable benchmark catalyst.

2 Experimental

2.1 Materials

The Al_2O_3 support and (0.7% w/w) Pt/Al_2O_3 were purchased from Puralox (Condea Vista. Co.) and Alfa Aesar, respectively. The gold precursor ($HAuCl_4$; 99.999%, Sigma-Aldrich) and urea (≥ 99%; Riedel-de Häen) were used as received. All the gases used (H_2, N_2, O_2 and He) were of high purity (99.9%, BOC gases). The reactants (*p*-methoxybenzaldehyde, *p*-tolualdehyde, benzaldehyde, benzyl alcohol and *p*-cyanobenzaldehyde; ≥ 98%, Aldrich; *p*-formylphenyl acetonitrile, 96.5%, Apollo Scientific) and solvents (ethanol, butanol, pentanol; ≥ 99.5%, Aldrich) were used as supplied without further purification.

2.2 Catalyst Preparation and Activation

A 1% w/w Au/Al_2O_3 was prepared by deposition–precipitation using urea as basification agent. An aqueous mixture of urea (tenfold excess) and $HAuCl_4$ in water (100 cm^3, 25×10^{-3} g cm^{-3}, pH = 2) was added to the support (ca. 10 g). The suspension was stirred and heated to 353 K (at 2 K min^{-1}) and the pH progressively increased to ca. 7 after 3 h as a result of thermally induced urea decomposition.

$$NH_2 - CO - NH_2 + 3H_2O \xrightarrow{T=353\,K} 2NH_4^+ + 2OH^- + CO_2 \quad (1)$$

The solid obtained was separated by centrifugation, washed with deionised water (with centrifugation between each washing) and dried in He (45 cm^3 min^{-1}) at 2 K min^{-1} to 373 K, which was maintained for 5 h. Au/Al_2O_3 and Pt/Al_2O_3 were crushed and sieved to 75 µm average particle diameter (ATM fine test sieves) and activated in 60 cm^3 min^{-1} H_2 at 2 K min^{-1} to 523 K (Au/Al_2O_3 [33]) and 773 K (Pt/Al_2O_3) [34]). Post activation, samples were cooled to 298 K and passivated in 1% v/v O_2/He for ex situ analysis.

2.3 Catalyst Characterisation

The metal (Au and Pt) content was measured by inductively coupled plasma-optical emission spectrometry (ICP-OES, Vista-PRO, Varian Inc.) from the (fivefold) diluted extract in HF (10 cm^3, 0.1 M). Catalyst activation and chemisorption (at 353 K) measurements were conducted using the commercial CHEM-BET 3000 (Quantachrome) unit. The sample was loaded into a U-shaped quartz cell (3.76 mm *i.d.*), heated in 17 cm^3 min^{-1} (Brooks mass flow controlled), 5% v/v H_2/N_2 at 2 K min^{-1} to 523–773 K and maintained until the signal returned to baseline. Samples were swept with 65 cm^3 min^{-1} N_2 for 1.5 h, cooled to 353 K and subjected to H_2 chemisorption using a pulse (10–50 µl) titration procedure. Hydrogen pulse introduction was repeated until the signal area was constant, indicating surface saturation. Metal particle morphology (size and shape) was determined by scanning transmission (JEOL 2200FS field emission gun-equipped TEM unit) electron microscopy (STEM), employing Gatan DigitalMicrograph 1.82 for data acquisition/manipulation. Samples were dispersed in acetone and deposited on a holey carbon/Cu grid (300 Mesh). Up to 1000 individual particles were counted and the surface area mean metal (Au, Pt) diameter (d_{STEM}) calculated from

$$d_{STEM} = \frac{\sum_i n_i d_i}{\sum_i n_i} \tag{2}$$

where n_i is the number of particles of diameter d_i.

2.4 Catalytic System

The liquid phase hydrogenation reactions ($T = 353$ K; $P = 9.0$ bar) were carried out in a commercial batch stirred stainless steel reactor (100 cm^3 autoclave, Parr reactor) equipped with a H_2 supply system (GCE-Druva). The temperature was maintained at 353 ± 1 K using a process controller (Scientific & Medicine Products Ltd). At the beginning of each run, the aldehyde (or benzyl alcohol) solution (40 cm^3 of pentanol, butanol, ethanol, H_2O or ethanol + H_2O; 0.05 M) and catalyst were charged and flushed three times with N_2. The system was heated to the reaction temperature, pressurised and the stirring engaged (time $t = 0$ for reaction). In a series of blank tests, there was negligible conversion in the absence of catalyst or without H_2. The initial molar reactant to metal ratio spanned the range 2×10^3–11×10^3. A liquid sampling system via syringe with in-line filters allowed a controlled withdrawal of aliquots (≤ 1.0 cm^3) from the reactor. The concentration of reactant/product was determined from the total mass balance in the reaction mixture. Fractional conversion of benzaldehyde ($X_{Benzaldehyde}$) is defined as

$$X_{Benzaldehyde\ (-)} = \frac{C_{Benzaldehyde,0} - C_{Benzaldehyde}}{C_{Benzaldehyde,0}} \tag{3}$$

where subindex '0' refers to initial concentration. Benzaldehyde consumption rate (R, mol mol_{metal}^{-1} h^{-1}) was determined from a linear regression of the temporal benzaldehyde concentration profiles at $X_{Benzaldehyde} < 0.35$ [35] according to:

$$R\ (\text{mol mol}_{metal}^{-1}\ \text{h}^{-1}) = \left(\frac{\Delta C_{Benzaldehyde}}{\Delta t}\right) \cdot \left(\frac{1}{n_{metal}}\right) \tag{4}$$

where n_{metal} is the metal concentration (mol_{metal} cm^{-3}). Turnover frequency (TOF, s^{-1}) was calculated using metal dispersion measurements from STEM as described elsewhere [36]. Selectivity to benzyl alcohol ($S_{Benzyl\ alcohol}$) is given by

$$S_{Benzyl\ alcohol}\ (\%) = \frac{C_{Benzyl\ alcohol}}{C_{Benzaldehyde,0} - C_{Benzaldehyde}} \times 100 \tag{5}$$

Product composition was determined by gas chromatography using a Perkin-Elmer AutoSystem XL chromatograph equipped with a programmed split/splitless injector and a flame ionisation detector, employing a DB-1 capillary column (*i.d.* = 0.33 mm, length = 50 m, film thickness = 0.20 µm). Data acquisition and manipulation were performed using the TotalChrom Workstation (Version 6.3.2 for Windows) chromatography data system. Repeated reaction runs with the same batch of catalyst delivered raw data reproducibility and carbon mass balances within ± 5%.

3 Results and Discussion

3.1 Catalyst Characterisation

The metal loading, particle size (from STEM analysis) and H_2 chemisorption values are given in Table 1. Both supported catalysts exhibit similar loading where the metal phase takes the form of pseudo-spherical particles (Fig. 1I) over the 1–8 nm size range (Fig. 1II). This equivalence permits a direct comparison of catalytic response. Hydrogen uptake on supported Au is sensitive to metal size and

Table 1 Metal content, mean metal particle size from STEM analysis (d_{STEM}), H_2 chemisorption (at 353 K) and catalytic activity expressed as reaction rate (R) and turnover frequency (TOF) in the liquid phase hydrogenation of benzaldehyde (using water as solvent): $T = 353$ K; $P = 9$ bar

	Au/Al_2O_3	Pt/Al_2O_3
Metal content w/w (%)	1.1	0.7
d_{STEM} (nm)	3.6	1.7
H_2 uptake (μmol g^{-1})	2.8	22.7
R (mol mol^{-1}_{metal} h^{-1})	78	446
$TOF \times 10^{-3}$ (s^{-1})	65	186

dissociative adsorption is favoured on smaller (1–10 nm) particles [37]. The eightfold lower H_2 uptake on Au/Al_2O_3 relative to Pt/Al_2O_3 (Table 1) can be linked to the high activation barrier for H_2 adsorption on Au [38] and greater capacity of Pt to dissociate H_2 [39, 40].

3.2 Liquid Phase Hydrogenation of Benzaldehyde

Reaction selectivity is challenging in benzaldehyde hydrogenation [1–6, 9, 13] with possible by-products, as shown in Scheme 1. Step I represents the target carbonyl group reduction. Subsequent hydrogenolysis results in the formation of benzene (step II) and toluene (step III) [41, 42]. Benzene and toluene can also be formed directly from benzaldehyde (steps IV and V) [41]. Further hydrogenation of benzyl alcohol to cyclohexylmethanol (step VI) has been reported for reaction over Ru/C [43] with toluene reduction to methylclohexane (step VII) over Ni/Al_2O_3 [6]. Under all reaction conditions used in this study, benzaldehyde was converted solely to the target benzyl alcohol over Au/Al_2O_3.

3.2.1 Reaction Under Kinetic Control

Benzaldehyde hydrogenation rate was determined from the linear variation of concentration with time, as shown in Fig. 2I. We carried out a series of tests in order to minimise diffusion and mass transfer limitations and ensure the reaction was operated under kinetic control. The effect of variations in agitation speed (Fig. 2IA) and catalyst mass (Fig. 2IB) on reaction rate was examined as two well-established diagnostic tests to assess external and internal transfer constraints [44]. An increase in stirring speed from 300 to 700 rpm was accompanied by a proportional increase in rate.

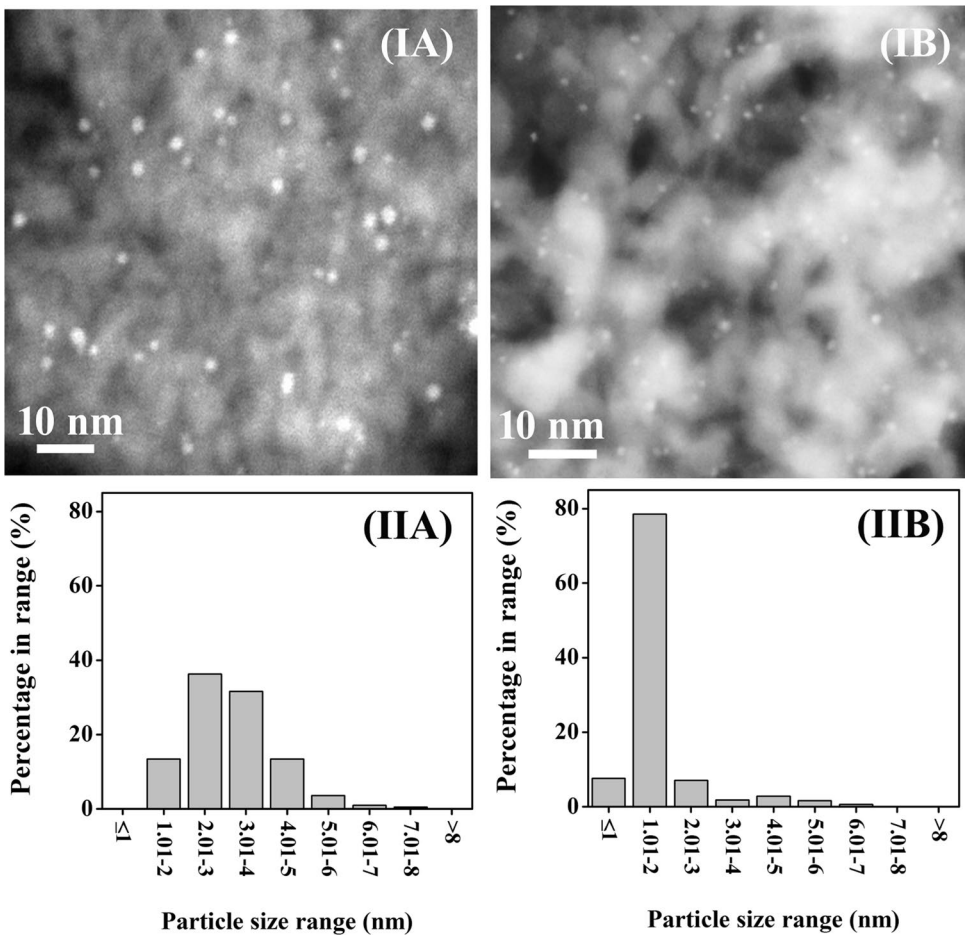

Fig. 1 **I** Representative STEM images with **II** associated particle size distribution for (**A**) Au/Al_2O_3 and (**B**) Pt/Al_2O_3

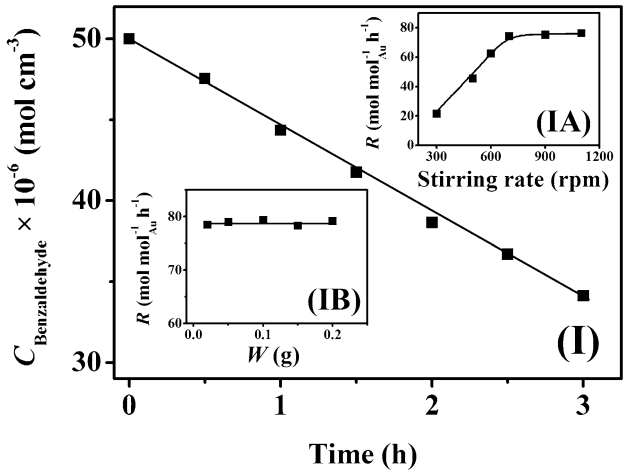

Fig. 2 **I** Variation of benzaldehyde concentration in water ($C_{Benzaldehyde}$, mol cm^{-3}) with time; dependence of benzaldehyde consumption rate (R, mol mol$^{-1}_{Au}$ h^{-1}) with **(IA)** stirring speed and **(IB)** mass of catalyst (W, g) for reaction over Au/Al_2O_3. *Note*: Solid lines provide a guide to aid visual assessment. *Reaction conditions*: $T = 353$ K, $P = 9$ bar

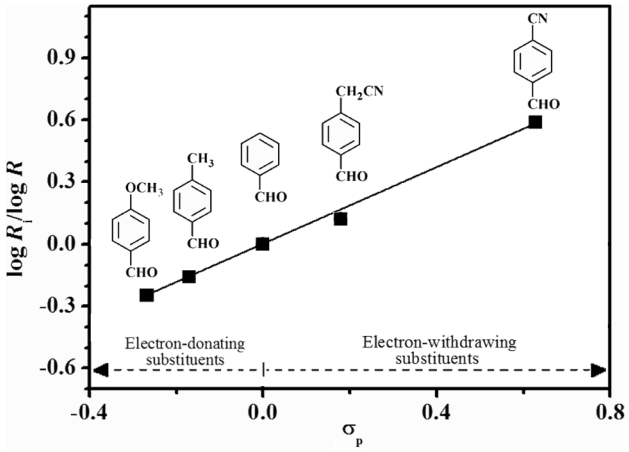

Fig. 3 Hammett plot for the selective –C=O group reduction of *para*-substituted benzaldehydes over Au/Al_2O_3 at $T = 353$ K and $P = 9$ bar. *Note*: Solid line represents fit to Eq. (6)

Rate remained constant > 700 rpm, indicative of minimal gas–liquid/liquid–solid mass transfer contributions to overall rate [45]. Based on these results, the stirring speed was set at 900 rpm for subsequent tests. Rate was invariant over the range of catalyst masses considered in this work, confirming chemical control where external or internal transport constraints do not contribute to the catalytic response [45].

3.2.2 Reaction Mechanism and Solvent Effects

The effect of ring substituents was considered by testing the hydrogenation of substituted benzaldehydes bearing electron donating and withdrawing substituents (–OCH_3, –CH_3, –CH_2CN, –CN) in the *para* position. In each case, Au/Al_2O_3 showed full selectivity to the corresponding alcohol with decreasing activity in the order: *p*-cyanobenzaldehyde > *p*-formylphenyl acetonitrile > benzaldehyde > *p*-tolualdehyde > *p*-methoxybenzaldehyde. The rate data were subjected to a Hammett correlation in order to probe reaction mechanism [46]. Rate for the substituted benzaldehyde (R_i) is related to benzaldehyde as reference (R) according to

$$\log\left[\frac{R_i}{R}\right] = \rho \times \sigma_p \tag{6}$$

The reaction constant (ρ) provides a measure of the susceptibility to substituent electronic effects while the σ_p factor is an empirical parameter (values taken from [46]) that reflects substituent electron donating/acceptor character [47, 48]. The fit of the experimental rate data is presented in Fig. 3. The low ρ (0.9) extracted from the linear correlation is close to that (0.7) reported for liquid phase hydrogenation of acetophenones over Pd/C [49] and suggests a partial charge in the transition state [7]. A positive reaction constant is consistent with nucleophilic addition [50]. Hydrogen can undergo heterolytic dissociation on the surface of Au/Al_2O_3 to generate H^- that bonds to Au [16]. The hydride ion (H^-) supplied by Au acts as a nucleophile that attacks the positively charged carbon in the –C=O group, activated on support Lewis acid sites (Al^{3+}) at the interface with the metal [51]. An electron-donating substituent (in the *para*-position) lowers the reactivity of the carbonyl-carbon which, in turns, lowers the rate of reaction.

The solvent serves to dissolve the reactant and/or products but can also interact with the catalyst and influence performance [45]. Benzaldehyde hydrogenation rate was lower in ethanol (23 mol mol$^{-1}_{Au}$ h^{-1}) relative to water (78 mol mol$^{-1}_{Au}$ h^{-1}). The higher rate in aqueous solution can not be due to H_2 solubility as under reaction conditions ($T = 353$ K, $P = 9$ bar) solubility is higher in ethanol (3.7 μmol cm^{-3}) than water (0.8 μmol cm^{-3}) [25]. The dielectric constant (ε) provides a measure of solvent capacity to interact with charged surface sites [52]; ε for water + ethanol mixtures was calculated following the approach described previously [25]. An increase in rate with solvent dielectric constant (ε) is shown in Fig. 4. Competition of solvent and benzaldehyde for adsorption sites [53] can impact on hydrogenation rate where increased surface affinity for the solvent inhibits benzaldehyde activation, resulting in lower reaction rate. Water [54] and alcohols [55] can adsorb on Lewis acid sites through the oxygen of the hydroxyl group and the greater electron density of the hydroxyl oxygen in alcohols must result in a stronger interaction that increases with increasing alcohol chain length [56].

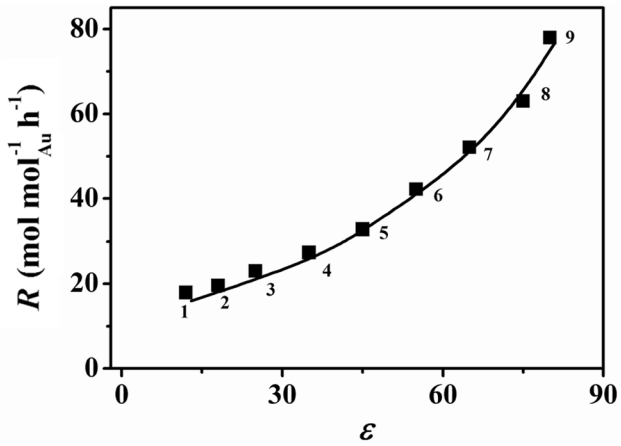

Fig. 4 Benzaldehyde hydrogenation rate (R, mol mol_{Au}^{-1} h^{-1}) over Au/Al_2O_3 as a function of solvent dielectric constant (ε) for reaction in (1) pentanol; (2) butanol; (3) ethanol; ethanol:H_2O = (4) 5:1; (5) 3:1; (6) 1:1; (7) 0.8:1; (8) 0.6:1; (9) H_2O. *Note*: Solid line provides a guide to aid visual assessment. *Reaction conditions*: T = 353 K, P = 9 bar

The solvent can also influence reactant activation through hydrogen bonding with the –C=O function [28, 29]. This results in charge transfer from the lone pair of the oxygen atom in the carbonyl group to the O–H bond in protic solvents [57], the carbonyl-carbon becomes more electrophilic and the rate of reaction increases. Akpa et al. [58] employed DFT calculations to investigate 2-butanone hydrogenation in water over Ru/SiO_2 and concluded that strong interaction between water and 2-butanone lowered the activation energy barrier and enhanced reaction rate. Catalyst (Ru/C) testing has also shown higher 2-butanone hydrogenation rate in solvents with higher ε [28]. In contrast, Bertero et al. [27] and Aramendía et al. [30] using Ni/SiO_2 and Pd/$AlPO_4$, respectively, reported a decrease in acetophenone hydrogenation rate with increasing ε due to solvation that inhibited the adsorption step.

3.2.3 Au/Al_2O_3 versus Pt/Al_2O_3

The reaction rate (and *TOF*) recorded for Pt/Al_2O_3 was significantly higher (Table 1), which can be attributed to the greater H_2 chemisorption capacity. Reaction over Au/Al_2O_3 exhibited full selectivity to the target alcohol at all levels of benzaldehyde conversion (Fig. 5I) to deliver 100% benzyl alcohol yield. This response was probed further by considering benzyl alcohol hydrogenation over Au/Al_2O_3; no conversion was detected. The benchmark Pt/Al_2O_3 promoted hydrogenolysis to toluene and benzene with a lower yield (95%) to benzyl alcohol at full benzaldehyde conversion. The reaction was prolonged for a further 15 h after complete benzaldehyde conversion (Fig. 5II). Conversion of benzyl alcohol (to toluene and benzene) over Pt/Al_2O_3 resulted in a temporal decline in selectivity to the alcohol. This suggests sequential hydrogenation (step I, Scheme 1) and hydrogenolysis (steps II and III) steps. In contrast, full selectivity to benzyl alcohol was maintained with Au/Al_2O_3 over extended reaction times with no measurable hydrogenolysis. The results from this work illustrate the potential of supported Au for the selective transformation of substituted benzaldehydes with 100% yield of the target alcohol over prolonged reaction times.

4 Conclusions

The liquid phase (T = 353 K, P = 9.0 bar) hydrogenation of benzaldehyde over (1% w/w) Au (mean size = 3.6 nm) on Al_2O_3 was fully selective with 100% yield of the target benzyl alcohol. Exclusive –C=O reduction extended to a range of *p*-substituted (–OCH_3, –CH_3, –CH_2CN, –CN) benzaldehydes. The reaction proceeds via a nucleophilic mechanism where electron withdrawing ring substituents elevated rate as demonstrated by the linear Hammett relationship. Selective hydrogenation rate increased with increasing solvent dielectric constant (ε), which is accounted for in terms of: (i) competition

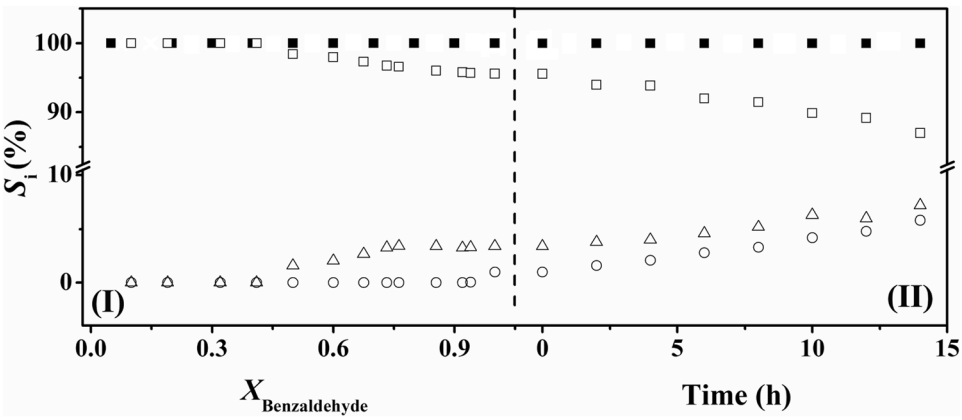

Fig. 5 Selectivity (S_i, %) as a function of **(I)** benzaldehyde fractional conversion ($X_{Benzaldehyde}$) and **(II)** time, after 100% conversion of benzaldehyde (in water) had been reached over Au/Al_2O_3 (solid symbols) and Pt/Al_2O_3 (open symbols); benzyl alcohol (open square, filled square), benzene (open triangle) and toluene (open circle). *Reaction conditions*: T = 353 K, P = 9 bar

for surface adsorption sites that is more pronounced for alcohols with lower ε; (ii) reactant solvation by solvents with higher ε that activates –C=O for nucleophilic attack. Reaction over a Pt/Al_2O_3 benchmark (mean Pt size = 1.7 nm) was non-selective with the formation of by-products from hydrogenolysis. A higher consumption rate recorded for Pt/Al_2O_3 can be attributed to greater H_2 chemisorption capacity. Our results demonstrate the potential of Au for ultra-selective aldehyde to alcohol hydrogenation using water as solvent.

Acknowledgements The authors are grateful to Dr. Maoshuai Li for his contribution to the project. This work received support from the Overseas Research Students Award Scheme (ORSAS) to Dr. Y. Hao and the Engineering and Physical Sciences Research Council EPRSC (Grant Number EP/L016419/1 to Chiara Pischetola through CRITICAT program). We also acknowledge EPSRC support for free access to the TEM/SEM facility at the University of St Andrews.

Compliance with Ethical Standards

Conflict of interest The authors declare no conflicts of interest.

References

1. Bhanushali JT, Kainthla I, Keri RS, Nagaraja BM (2016) ChemistrySelect 1:3839
2. Song L, Li K, Li X, Wu P (2011) React Kinet Mech Catal 104:99
3. Pinna F, Menegazzo F, Signoretto M, Canton P, Fagherazzi G, Pernicone N (2001) Appl Catal A 219:195
4. Divakar D, Manikandan D, Kalidoss G, Sivakumar T (2008) Catal Lett 125:277
5. Liu S, Fan X, Yan X, Du X, Chen L (2011) Appl Catal A 400:99
6. Saadi A, Merabti R, Rassoul Z, Bettahar MM (2006) J Mol Catal A 253:79
7. Saadi A, Rassoul Z, Bettahar MM (2000) J Mol Catal A 164:205
8. Li X, Zheng W, Pan H, Yu Y, Chen L, Wu P (2013) J Catal 300:9
9. Han M, Zhang H, Du Y, Yang P, Deng Z (2011) React Kinet Mech Catal 102:393
10. Ding Y, Li X, Li B, Wang H, Wu P (2012) Catal Commun 28:147
11. Li X, Shen Y, Song L, Wang H, Wu H, Liu Y, Wu P (2009) Chem Asian J 4:699
12. Perret N, Cárdenas-Lizana F, Keane MA (2011) Catal Commun 16:159
13. Arai M, Obata A, Nishiyama Y (1997) J Catal 166:115
14. Bond GC (2016) Gold Bull 49:53
15. Pan M, Brush AJ, Pozun ZD, Ham HC, Yu W-Y, Henkelman G, Hwang GS, Mullins CB (2013) Chem Soc Rev 42:5002
16. Mitsudome T, Kaneda K (2013) Green Chem 15:2636
17. Cárdenas-Lizana F, Keane MA (2014) Towards chemoselectivity: the case of supported Au for hydrogen mediated reactions. In: Prati L, Villa A (eds) Gold catalysis: preparation, characterization and applications in the gas and liquid phase. Pan Stanford Publ, Singapore, pp 415–465
18. Zhimin L, Hadi A, Chao L, Gao L (2017) Curr Org Chem 21:476
19. Zhao J, Jin R (2018) Nano Today 18:86
20. Hari TK, Yaakob Z (2015) Chin J Chem Eng 23:327
21. Lenz J, Campo BC, Alvarez M, Volpe MA (2009) J Catal 267:50
22. Milone C, Tropeano ML, Gulino G, Neri G, Ingoglia R, Galvagno S (2002) Chem Commun 8:868
23. Mohr C, Hofmeister H, Claus P (2003) J Catal 213:86
24. Zanella R, Louis C, Giorgio S, Touroude R (2004) J Catal 223:328
25. Gómez-Quero S, Cárdenas-Lizana F, Keane MA (2010) AIchE 56:756
26. Drelinkiewicza A, Waksmundzka A, Makowski W, Sobczak JW, Król A, Zieba A (2004) Catal Lett 94:143
27. Bertero NM, Trasarti AF, Apesteguía CR, Marchi AJ (2011) Appl Catal A 394:228
28. Wan H, Vitter A, Chaudhari RV, Subramaniam B (2014) J Catal 309:174
29. Ren B, Zhao M, Dong L, Li G (2014) Catal Commun 50:92
30. Aramendía MA, Borau V, Gómez JF, Herrera A, Jiménez C, Marinas JM (1993) J Catal 140:335
31. Okamoto M, Hirao T, Yamaai T (2010) J Catal 276:423
32. Wang M-M, He L, Liu Y-M, Cao Y, He H-Y, Fan K-N (2011) Green Chem 13:602
33. Mustafin K, Cárdenas-Lizana F, Keane MA (2017) J Chem Technol Biotechnol 92:2221
34. Kim SS, Lee HH, Hong SC (2012) Appl Catal A 423–424:100
35. Gómez-Quero S, Cárdenas-Lizana F, Keane MA (2008) Ind Eng Chem Res 47:6841
36. Li M, Wang X, Perret N, Keane MA (2014) Catal Commun 46:187
37. McEwan L, Julius M, Roberts S, Fletcher JCQ (2010) Gold Bull 43:298
38. Wang X, Perret N, Keane MA (2013) Appl Catal A 467:575
39. Hammer B, Nørskov JK (1995) Nature 376:238
40. Bus E, Miller JT, Bokhoven JAV (2005) J Phys Chem B 109:14581
41. Haffad D, Kameswari U, Bettahar MM, Chambellan A, Lavalley JC (1997) J Catal 172:85
42. Vannice MA, Poondi D (1997) J Catal 169:166
43. Kluson P, Cerveny L (1996) J Mol Catal A 108:107
44. Renken A, Kiwi-Minsker L (2012) Catalytic reaction: engineering principles. Willey, Weinhem
45. Singh UK, Vannice MA (2001) Appl Catal A 213:1
46. Jaffé HH (1953) Chem Rev 53:191
47. Shorter J (2000) Chem Lysty 94:210
48. Johnson CD (1973) The hammett equation. Cambridge University Press, Cambridge
49. Bekkum Hv, Kieboom APG, Putte KJGvD (1969) Reccl Trav Chim Pay B 88:52
50. Qu H-E, Xiao C, Wang N, Yu K-H, Hu Q-S, Liu L-X (2011) Molecules 16:3855
51. Milone C, Trapani MC, Galvagno S (2008) Appl Catal A 337:163
52. Reichardt C (2004) Solvents and solvent effect in organic chemistry. Wiley, New York
53. Drexler MT, Amiridis MD (2003) J Catal 214:136
54. Menetrey M, Markovits A, Minot C (2003) Surf Sci 524:49
55. Cai S, Sohlberg K (2003) J Mol Catal A 193:157
56. Walz MM, Werner J, Ekholm V, Prisle NL, Ohrwall G, Bjorneholm O (2016) Phys Chem Chem Phys 18:6648
57. Kumar VR, Verma C, Umapathy S (2016) J Chem Phys 144(064302):1
58. Akpa BS, D'Agostino C, Gladden LF, Hindle K, Manyar H, McGregor J, Li R, Neurock M, Sinha N, Stitt EH, Weber D, Zeitler JA, Rooney DW (2012) J Catal 289:30